Machinability of Cast Iron

AUTHOR(S):

OKUSHIMA, Keiji; IWATA, Kazuaki; NAKATOMI, Itsuro; KURIMOTO, Takeshi

CITATION:

OKUSHIMA, Keiji ...[et al]. Machinability of Cast Iron. Memoirs of the Faculty of Engineering, Kyoto University 1962, 24(3): 301-314

ISSUE DATE:

1962-08-31

URL:

http://hdl.handle.net/2433/280528

Machinability of Cast Iron

By

Keiji OKUSHIMA*, Kazuaki IWATA*, Itsuro NAKATOMI*
and Takeshi KURIMOTO*

(Received April 30, 1962)

The machinability of cast iron was investigated from the standpoint of chip formation, tool life, and surface finish.

Cutting mechanisms of cast iron were analysed based upon the flow region concept. The effects of feed and rake angle on the cutting process were discussed.

The most suitable tool material for cutting cast iron was selected and effects of cutting conditions on tool life were investigated over a wide range.

Machinability based upon surface finish is discussed in connection with tool wear.

1. Introduction

Cast iron consists of graphite, ferrite, pearlite, sorbite, cementite, steadite, and non-metallics (such as sand, manganese sulfide, silicates, oxides, etc.). For this reason various investigations have been made regarding the machinability of this material, and as a result it was found that important factors which affect the machinability of cast iron are mainly microstructure and grain size[1,2].

The machinability is investigated and discussed for each type of microstructure, for instance, grey cast iron, special cast iron, chilled cast iron, and nodular cast iron etc.[3,4].

In this paper, machinability of grey cast iron was investigated from the standpoint of chip formation based upon the flow region concept. Then tool life test was performed and surface roughness was measured at various cutting times. The experimental results on the relationship between tool wear and surface finish is discussed.

2. Experimental procedure

Grey cast iron was used for the present experiment. The chemical composition of this work material is shown in Table 1. Orthogonal cutting and

* Department of Precision Mechanics

Table 1. Chemical composition of test material.

Chemical composition	C	Si	Mn	P	S	Ni	Cr	Cu	Mo
Content	2.78	1.28	0.53	0.17	0.094	Nil	Nil	Trace	0.04

conventional cutting (three-dimensional cutting) tests were carried out in order to investigate the machinability of cast iron from the standpoint of chip formation, tool life, and surface finish.

The following machine tool and cutting tools were used.

Machine tool — High-speed lathe (Niigata Iron Works)

Tool materials

(a) Orthogonal cutting — Carbite tool grade H-1 (JIS 33-3)

Tool geometry

Back rake angle	0 deg.
Side rake angle	5 deg.
End relief angle	5 deg.
Side relief angle	5 deg.
End cutting edge angle	5 deg.
Side cutting edge angle	0 deg.
Nose radius	0.1 mm

(b) Conventional cutting — Carbide tool grade G-1F, G-2F, H-1, H-2, U-2, Titanium carbide (JIS 31-3)

Tool geometry

Back rake angle	0 deg.
Side rake angle	5 deg.
End relief angle	5 deg.
Side relief angle	5 deg.
End cutting edge angle	15 deg.
Side cutting edge angle	15 deg.
Nose radius	0.3 mm

Feed and depth of cut were altered as follows:

Feed;	0.16, 0.28, and 0.40 mm/rev.
Depth of cut;	1 and 3 mm

Since the surface layer of cast iron as received includes scales, sand, etc., the microstructure in this layer is different from the interior microstructure of the material. This layer was removed before the experiment.

Tool forces were measured with a three-component tool dynamometer of the strain gage type[5],

Ôkoshi's needle type optical roughness meter was used to measure the surface finish at various cutting times in order to investigate the effect of tool wear on surface finish.

3. Machinability evaluation from the standpoint of chip formation

(A) The analysis of the flow region area in discontinuous chip formation

The cutting mechanism producing a discontinuous type of chip was analysed based upon the flow region concept. According to this cutting process, the chip is produced by the plastic flow in a transitional deformation zone which exists between the work and the chip as shown in Fig. 1; that is, discontinuous chip

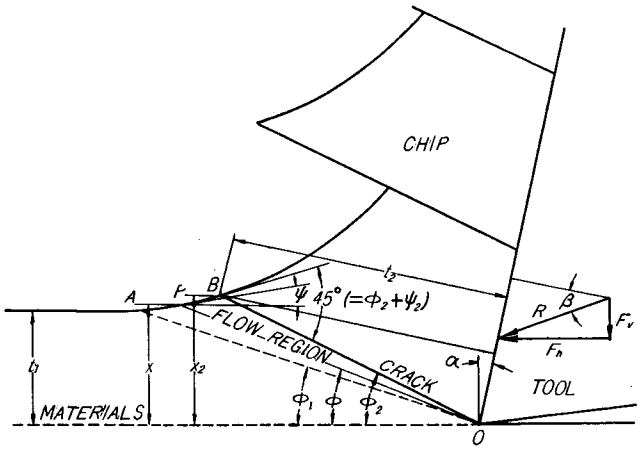

Fig. 1. Analysis of cutting mechanism of discontinuous chip formation based on flow region concept.

is produced when the shearing stress on the end boundary line of the flow region reaches the breaking limit of the work material.

Assuming that AB in Fig 1 is an approximately straight line, the flow region area S in discontinuous chip formation is expressed as follows:

$$S = \frac{1}{2} \cdot \frac{t_1 \cdot t_2}{\sin \phi_1 \cdot \cos (\phi_2 - \alpha)} \sin \varnothing \qquad \cdots\cdots(1)$$

where t_1; Depth of cut, mm
t_2; Thickness of chip, mm
α; Rake angle, deg.
$\varnothing$; Sector angle of the flow region, deg.
ϕ_1; Inclination angle of the starting boundary line of flow region, deg.

ϕ_2; Inclination angle of the end boundary line of the flow region, deg.

In this equation, inclination angles for the starting and ending boundary lines and the sector angle of the flow region were deduced thoretically as follows[6];

$$\phi_1 = \frac{1}{2}(K_1 - \beta + \alpha) \qquad \cdots\cdots(2)$$

$$\phi_2 = \frac{1}{2}(K_2 - \beta + 2\alpha) \qquad \cdots\cdots(3)$$

$$K_1 = \sin^{-1}\left\{\frac{2}{k_1}\sin\beta + \sin(\beta - \alpha)\right\} \qquad \cdots\cdots(4)$$

$$K_2 = \cos^{-1}\left\{\frac{2}{k_2}\sin\beta - \cos\beta\right\} \qquad \cdots\cdots(5)$$

$$k_1 = \frac{l}{t}, \quad k_2 = \frac{l}{t_2} \qquad \cdots\cdots(6)$$

$$\Phi = \phi_2 - \phi_1 = \frac{1}{2}(\alpha - K_1 + K_2) \qquad \cdots\cdots(7)$$

$$\tau_{0p} = \frac{R \cdot \sin\phi \cos(\phi - \alpha + \beta)}{bx} \qquad \cdots\cdots(8)$$

where R; Cutting force, Kg
b; Width of cut, mm
l; Tool-chip contact length, mm

(B) Experimental results and discussion

The cutting force (principal and thrust cutting components), thickness of chip and tool-chip contact length were measured when cutting cast iron with carbide grade H-1. The results are shown in Figs. 2 and 3. Fig. 2(a) and Fig.

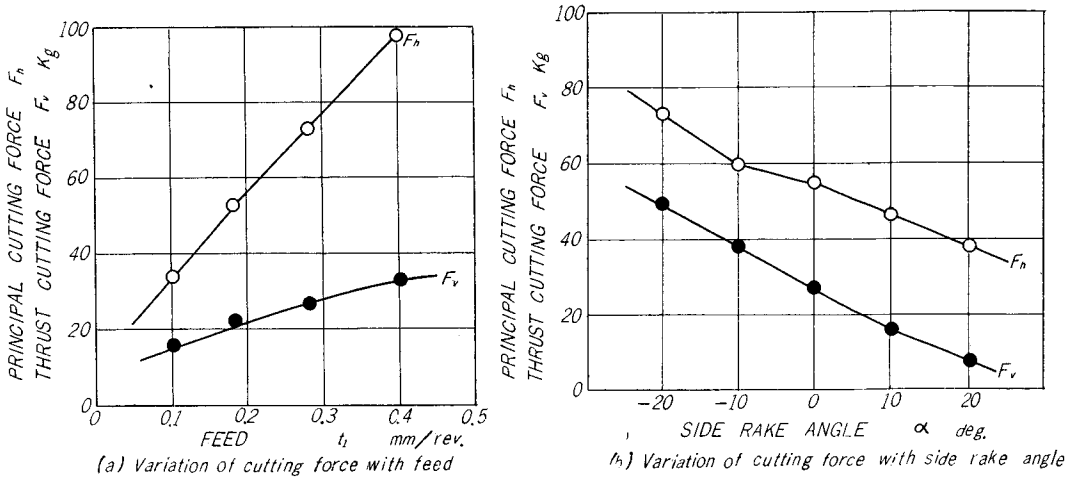

(a) Variation of cutting force with feed

(b) Variation of cutting force with side rake angle

Fig. 2. Variation of cutting force with feed and side rake angle.
Cutting conditions; cutting speed 95 m/min, depth of cut 2 mm; dry;

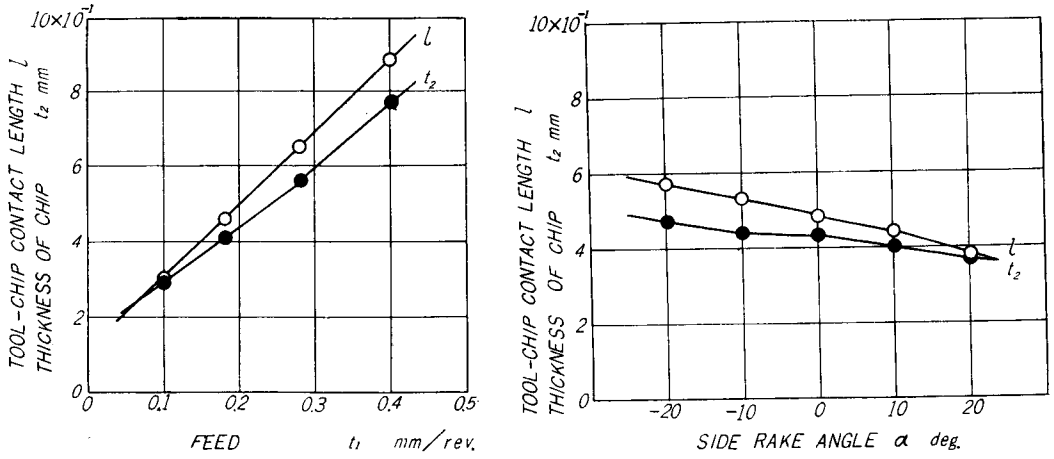

(a) Variation of tool-chip contact length and thickness of chip with feed

(b) Variation of tool-chip contact length and thickness of chip with side rake angle.

Fig. 3. Variation of tool-chip contact length and thickness of chip with feed and side rake angle.
Cutting conditions; cutting speed 95 m/min, depth of cut 2 mm; dry:

3(a) showing the effect of feed on cutting force, and thickness of chip and tool-chip contact length for the cutting speed of 95 m/min., the depth of cut of 2 mm and side rake angle of 5 deg. Fig. 2(b) and Fig. 3(b) show the effect of side rake angle on cutting force, thickness of chip and tool-chip contact length for the cutting speed of 95 m/min, depth of cut of 2 mm and feed of 0.18 mm/rev..

(a) The effect of feed

Using experimental data mentioned, various angle and stresses for cutting process were calculated from the above equations and are shown in Fig. 4(a), and (b) in relation to feed.

It was found that the inclination angle of the end boundary line of the flow region ϕ_2 and the sector angle of flow region $\varnothing$ increased in direct proportion to feed. Mean friction angle β decreased with an increase in feed. The inclination angle of the starting boundary line of the flow region ϕ_1 was constant. It is evident from this that the inclination angle of the starting boundary line ϕ_1 is smaller and that of the end boundary line ϕ_2 is larger than the conventional shear angle ϕ_0.

Shearing stress of starting boundary line of the flow region τ_1, compressive stresses of starting and end boundary lines of flow region σ_1, σ_2, and conventional compressive stress σ_0 show a tendency to decrease with an increase in feed, but conventional shearing stress τ_0 is almost constant (about 44 kg/mm^2).

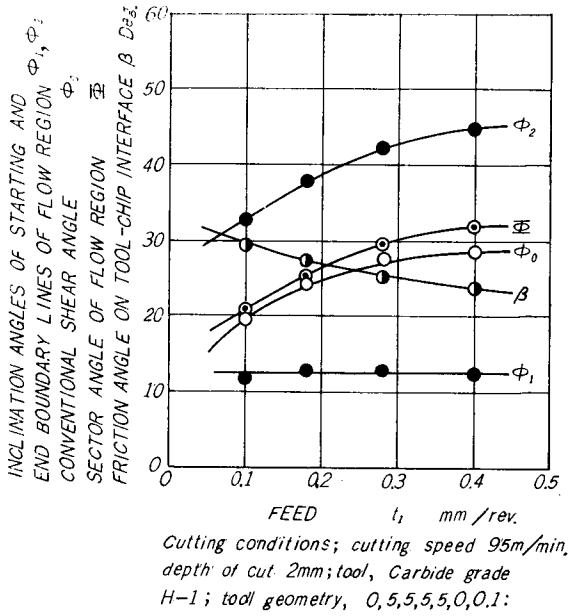

Fig. 4 (a). Calculation value of grey cast iron with feed.

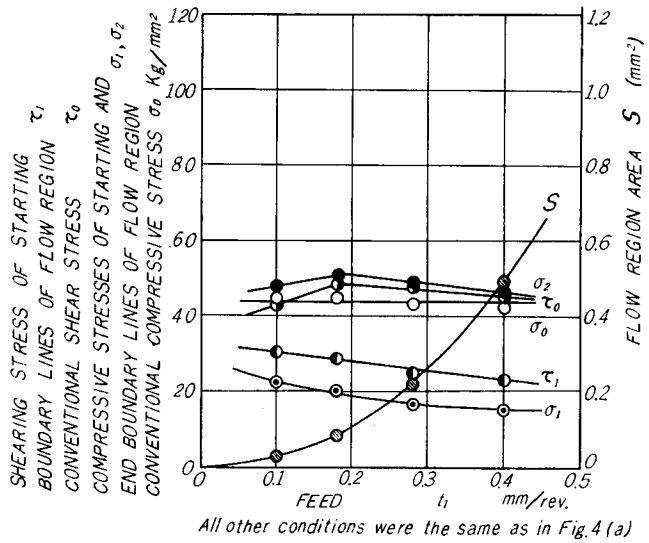

Fig. 4 (b). Calculation value of grey cast iron with feed.

Regarding compressive stress, it increases gradually, from σ_1 on the starting boundary line of the flow region, σ_0 on the conventional shear plane, and to σ_2 on the end boundary line of the flow region.

On the other hand, it is obvious that the flow region area S increases with an increase of feed.

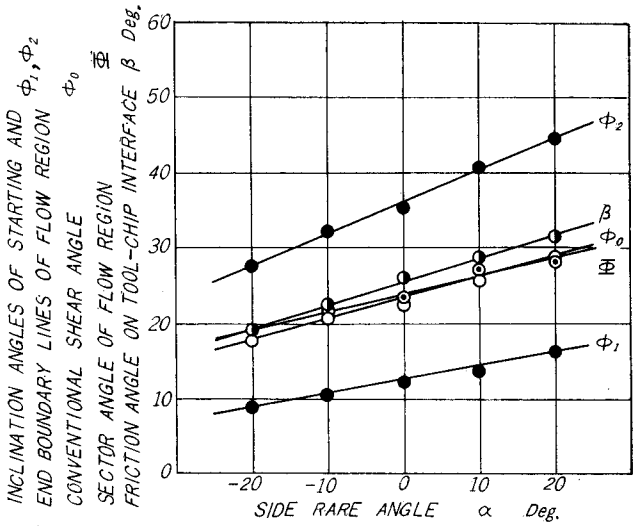

Cutting conditions; cutting speed 95 m/min., depth of cut 2mm, feed 0.18 mm/rev; tool. Carbide grade H-1; tool geometry, 0, var., 5, 5, 5, 0, 0.1; dry:

Fig. 5 (a). Calculation value of grey cast iron with side rake angle.

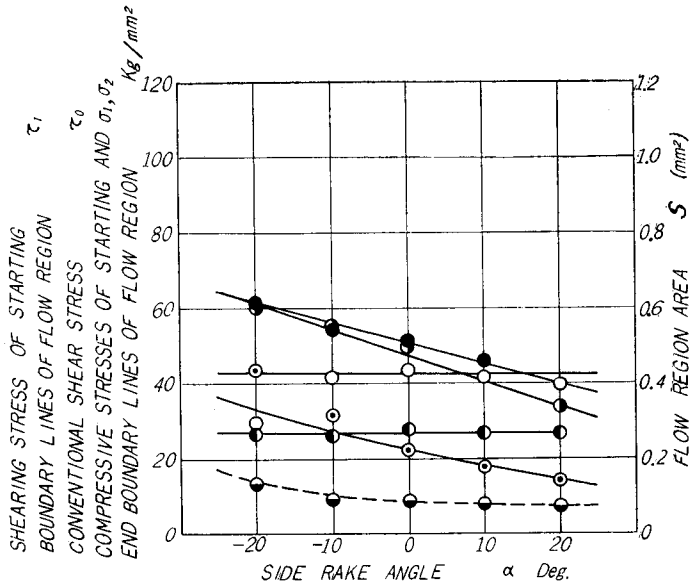

Fig. 5 (b). Calculation value of grey cast iron with side rake angle. All other conditions were the same as in Fig. 5 (a).

(b) The effect of side rake angle

Similar calculated values when changing the side rake angle as -20, -10, 0, 10, and 20 degree are shown in Fig. 5(a) and (b).

It is evident that ϕ_1, ϕ_2, ϕ_0, and β show a tendecy to increase with an increase in side rake angle, and $\varnothing$ increases gradually.

Compressive stresses σ_1, and σ_2 decrease with an increase in side rake angle, but τ_1 is almost constant.

It appears that the flow region area S decreases with an increase in side rake angle.

(c) Schematic cutting models

The schematic cutting models are shown in Fig. 6(a) and (b) in relation to feed and rake angle, respectively.

4. Machinability evaluation from the standpoint of tool life

A tool life test was run in order to select a suitable tool material for cutting cast iron.

Five grades of carbide and one grade of titanium carbide were used.

In this experiment, feed and depth of cut were kept constant, i.e., 0.28 mm/rev. and 1 mm respectively, and the cutting speed was varied.

Tool life data points are shown in Fig. 7(a) and (b). The criterion of tool life in this case was a flank wear of 0.3 mm or a crater wear of 0.05 mm.

It is evident from this that the most suitable tool material for cutting cast iron was grade U-2 of carbide and that the titanium carbide tool was excellent for protection of flank wear at low speeds. Regarding the cast iron cutting grade carbide, grade H-1 shows a better tool life and grade G-1F, and G-2F were worst. For crater wear, the titanium carbide tool showed a better tool life and grade H-2 was worst.

It appears that crater wear should be a criterion of tool life when cutting cast iron since crater wear was much grater than flank wear. Titanium carbide tools show a better tool life than carbide tools from the viewpoint of tool life, but the degree was not so obvious as in steel cutting. It is noted that in this case, flank wear was greater than crater wear.

The effect of cutting conditions on tool life was investigated in the following manner.

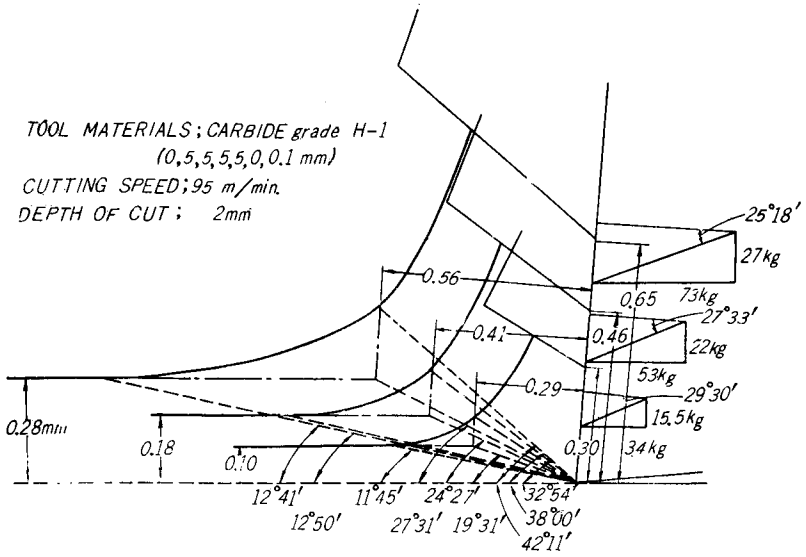

Fig. 6 (a). Schematic cutting madel for grey cast iron in terms of feed.

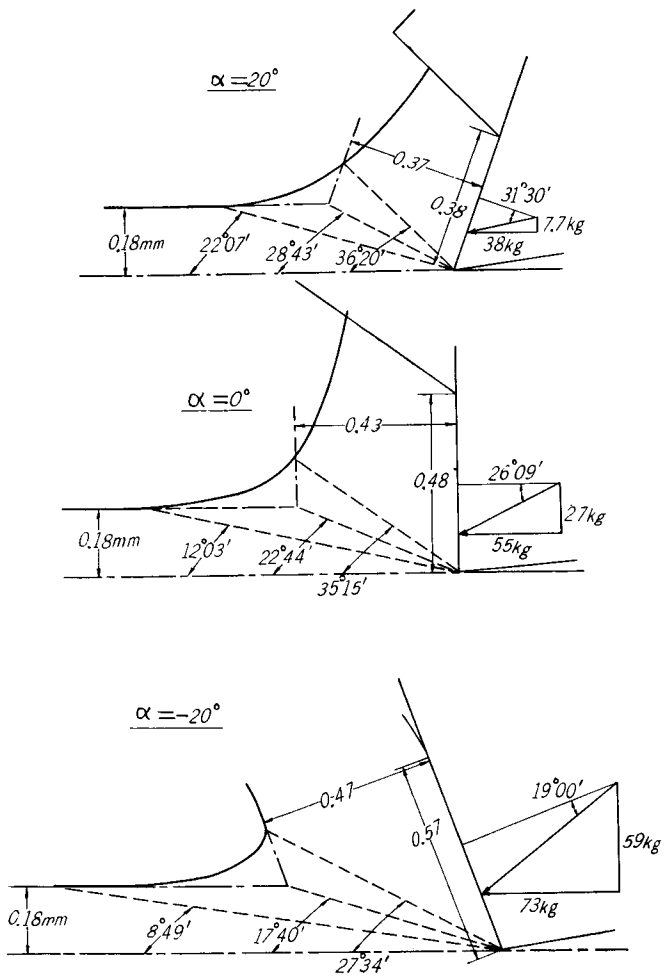

Fig. 6 (b). Schematic cutting model for grey cast iron in terms of side rake angle.

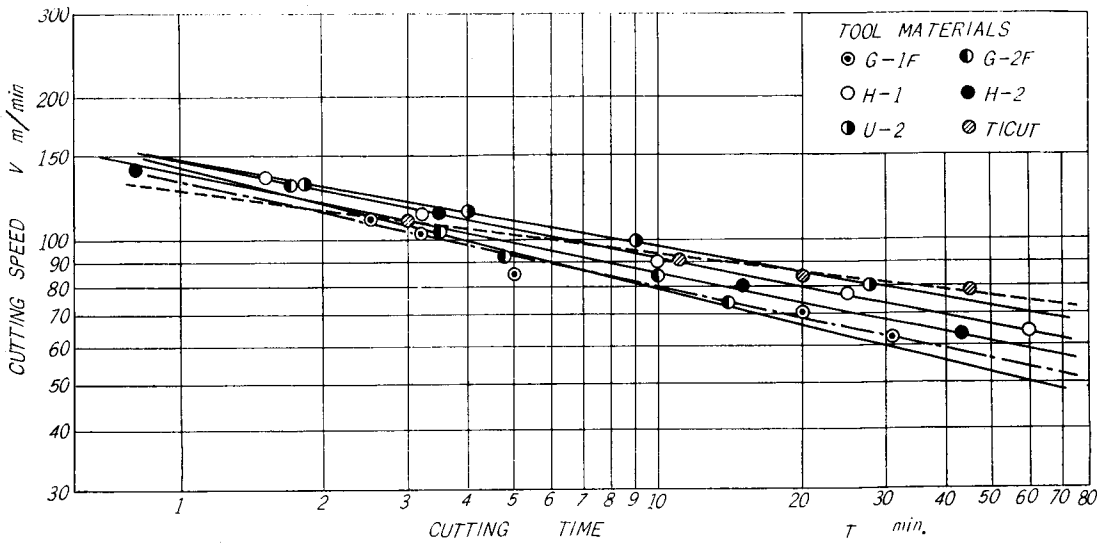

Fig. 7 (a). Tool life plots based upon the flank wear of grey cast iron for different tool materials Cutting conditions; feed 0.28 m/rev, depth of cut 1 mm, tool geometry, 0, 5, 5, 5, 15, 15, 0.3 mm; fluid, none:

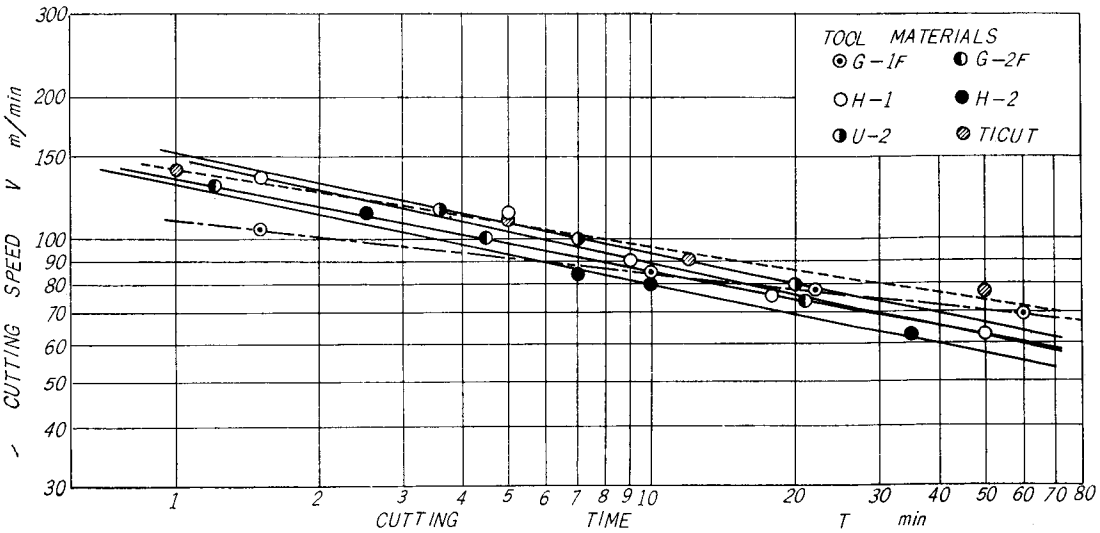

Fig. 7 (b). Tool life plots based upon the crater wear of grey cast iron for different tool materials. All other conditions were the same as in Fig. 7 (a)

The effect of feed on tool life is shown in Fig. 8. The criterion of tool life was a flank wear of 0.4 mm compared with 0.3 mm in the previous experiment, because flank wear was developed up to 0.3 mm for the initial cutting time for feed of 0.4 mm/rev..

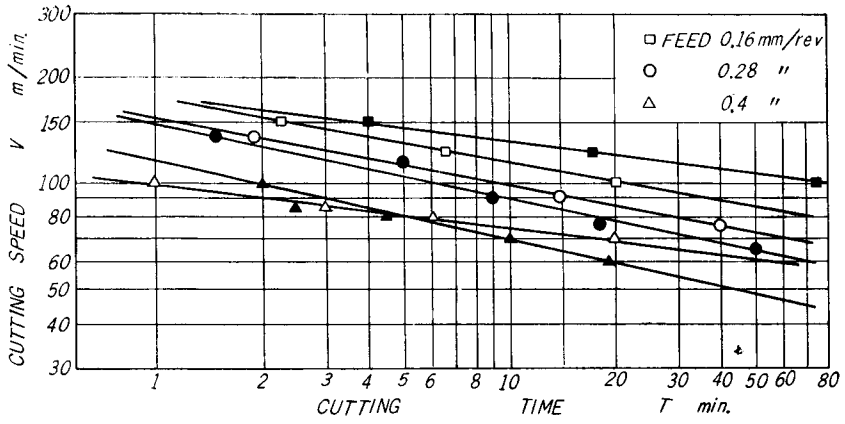

Fig. 8. Tool life plots of grey cast iron for feed.
Cutting conditions; depth of cut 1 mm, tool geometry, 0, 5, 5, 5, 15, 15, 0.3 mm; fluid none:
The criterion of tool life $V_B'=0.4$ mm, $K_T=0.05$mm

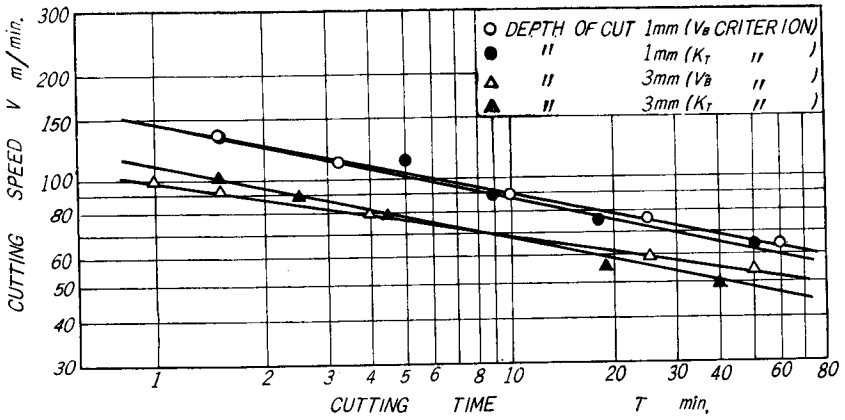

Fig. 9. Tool life plots of grey cast iron for depth of cut.
Cutting conditions; feed 0.28 mm/rev., tool geometry, 0, 5, 5, 5, 15, 15, 0.3 mm; fluid none:
The criterion of tool life $V_B'=0.3$ mm, $K_T=0.05$ mm

It is evident from Fig. 8 that the tool life is determined by crater wear for feed of 0.28 mm/rev. and by flank wear for feed of 0.16 mm/rev..

Fig. 9 shows the effect of depth of cut on tool life. An increase in depth of cut decreased tool life. It was observed that with the cutting speed of 30 min. tool life decreased about 30% when the depth of cut increased from 1 mm to 3 mm.

5. Machinability evaluation from the standpoint of surface finish (Especially, in relation to tool wear)

Surface roughness tests are generally associated with sharp cutting tools. However, in practice the cutting tool does not always remain sharp, but dulling is accompanied with tool wear.

Therefore, this point should be taken into consideration when machinability is discussed from the standpoint of surface finish.

In regard to this problem, Sada and Amano[7] discussed with cutting a high-carbon steel and a Cr-Mo steel.

In this section, a similar problem will be discussed in regard to cast iron. Fig. 10 shows the experimental data for surface finish in relation to cutting speed, using sharp cutting tools. The surface finish was found to be improved when cutting speed increased.

The maximum surface roughness in relation to the progress of flank wear of a cutting tool is shown in Fig. 11. In comparison with this data, S45C was tested in a similar way and the experimental data are shown in Fig. 12.

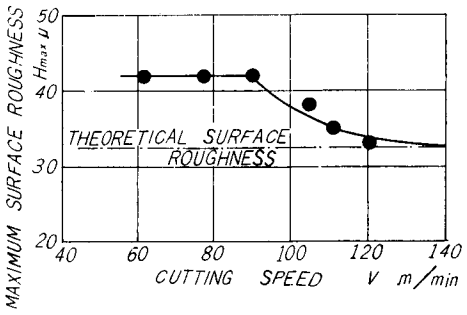

Fig. 10. The effect of cutting speed on surface roughness.

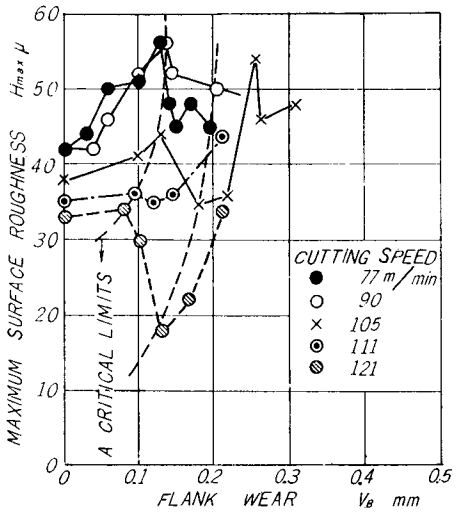

Fig. 11. Variation of maximum surface roughness with flank wear in cast iron cutting.

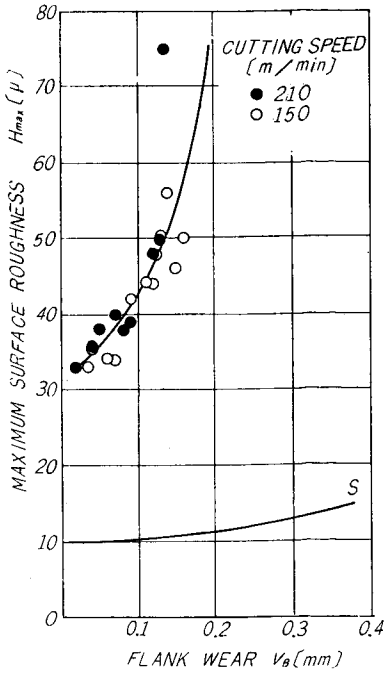

Fig. 12. Variation of maximum surface roughness with flank wear in S45C steel cutting.

Comparing Figs. 11 and 12, in the case of steel, the maximum surface roughness is almost the same for various cutting speeds and increases with tool wear and in the case of cast iron, the maximum surface roughness increases with tool wear as well as in the case of steel, but it decreases with a decrease in cutting speed.

Further, in the case of cast iron, the maximum surface roughness increases with an increase in tool wear until the tool wear reaches a certain limit, and it decreases with the progress of tool wear for the amount of tool wear over this limit.

The reason for this is as follows;

A main reason that the surface roughness increases with tool wear is considered to be that small chippings occur at the tool edge with the progress of cutting.

A reason that the surface roughness is improved after the tool wear reaches a critical limit is considered to be a variation in tool geometry.

Flank wear occurs mainly on the nose part, front relief face, and side relief face. It appears that the tool wear occuring on the nose part and the front relief face mainly affects surface finish when cutting cast iron.

Under the cutting conditions in this experiment, the maximum surface roughness is affected by nose radius, feed, and front cutting edge angle, and is expressed as follows;

$$H_{max} = r(1-\cos\varphi) + S\cdot\sin\varphi\cdot\cos\varphi - \sin\varphi\sqrt{S\cdot\sin\varphi(2r - S\cdot\sin\varphi)} \qquad (9)$$

where $S \geqq 2r\cdot\tan\varphi$

r; Nose radius, mm

φ; Front cutting edge angle, deg.

S; Feed, mm/rev.

Fig. 13 shows the relationship between maximum surface roughness and front cutting edge angle in terms of nose radius. It is found from this figure that the surface roughness decreases with a decrease in front cutting edge angle and an increase in nose radius.

Therefore, it is concluded that the surface roughness is improved with tool wear beyond the critical limit, since the nose radius increases and the front cutting edge angle decreases with the progress of tool wear as was observed in the experiment.

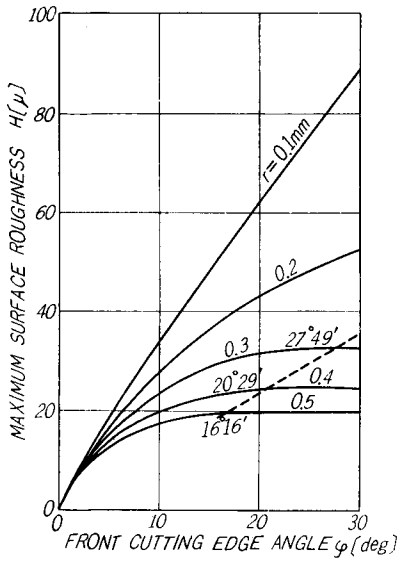

Fig. 13. The effect of front cutting edge angle on maximum surface roughness in terms to nose radius.

Surface roughness increased agiain for a large amount of tool wear when cutting cast iron as shown in Fig. 11. This is because the tool becomes dull and the vibration of the work material and the tool becomes noticiable for such a large amount of tool wear.

6. Conclusions

Machinability of cast iron was investigated from the standpoint of chip formation, tool life, and surface finish. This leads to the following conclusions.

(1) The cutting mechanism of cast iron was analyzed based upon the flow region concept. The effects of feed and the side rake angle on the cutting mechanism were discussed.

(2) The most suitable material when cutting cast iron was universal cutting grade of carbide U-2. Cast iron cutting grade of carbide, H-1 and titanium carbide were also effective.

(3) In cutting the cast iron, the maximum surface roughness increases with tool wear in the initial stage, but it decreases after the tool wear increases beyond a critical limit, and then it decreases again. This is explained by the variation of tool geometry due to wear on the nose part and front relief face of the end cutting edge.

References

1) Woldman & Gibbons: Machinability and machining of metals (1951) p. 228-260.
2) Michael Field & E. E. Stansbury: Trans. ASME (1947) p. 664.
3) Takeyama and others: J. S. Precision Mechanics 27-2 (1961) p. 39-44.
4) K. Hitomi & Thuring: Trans. ASME. S.B. vol. 83 (1961) p. 142-154.
5) K. Okushima and others: Trans. JSMA. 21, 110 (1955) p. 709-711.
6) K. Okushima & K. Hitomi: Trans. JSME 25, 150 (1959) p. 54-60.
7) T. Sada & Amano: J. S. Precision Mechanics 26-11 (1960).